Adsorption Properties of the Cu(115) Surface: Basic Interfaces

P.J. Godowski[a,*], A. Groso[b], S.V. Hoffmann[c] and J. Onsgaard[d]

[a]Institute of Experimental Physics, University of Wrocław, 50-204 Wrocław, Poland

[b]Ecole Polytechnique Fédérale de Lausanne, SB-SST CH J2 491 Station 6, Lausanne, Switzerland

[c]Institute for Physics and Astronomy, Aarhus University, DK-8000 Århus C, Denmark

[d]Department of Physics and Nanotechnology, Aalborg University, DK-9220 Aalborg Øst, Denmark

(Received December 21, 2009; in final form April 10, 2010)

The interfaces: K/Cu(115) and CO/Cu(115) have been characterized using surface sensitive techniques, including low energy electron diffraction and photoelectron spectroscopy. K adatoms show tendency to occupy the sites close to the step edges. At low temperature (near 125 K), after completion of two layers, potassium grows in 3D islands (the Stranski–Krastanov mode). At higher temperature, *e.g.* at room temperature, potassium introduces reconstruction of the substrate even at low coverages. Calibration of the alkali coverage, up to completion of the first layer, using the work function changes curve has been confirmed as a very convenient and precise procedure. The adsorbed state of CO at 130 K has been identified by registration of core levels obtained by the use synchrotron radiation photoelectron spectroscopy. The characteristics of the main 1*s* and satellite peaks have been analyzed in context of substrate geometry and compared with the ones of other copper planes. There are no indications of dissociative adsorption of CO, only residual carbon and oxygen were found after adsorbate desorption around 220 K. CO molecules show a strong tendency to "on top" adsorption in sites far from the step edges of the Cu(115) surface.

PACS numbers: 68.43.Fg, 68.55.Ac, 61.14.Hg, 79.60.Dp

1. Introduction

Stepped and modified metal surfaces have a very important role in catalytic reactions at the gas/solid interface. Due to the presence of different coordinated atoms, the step-related phenomena, as *e.g.* chemical reactivity at the steps, are enhanced at such places at the surfaces. On the other hand, the presence of alkali metals on the surfaces can seriously modify their reactivity as well. For these reasons the studies of adsorption properties of such interfaces are very well motivated from technological and scientific points of view.

The Cu(115) surface (fcc lattice) is composed of terraces of two and a half rows of atoms with the local square (001) symmetry separated by monoatomic steps with (111) orientation. The elementary surface cell is found to be 255.3×663.2 pm^2 and its geometrical structure has been discussed in detail in [1, 2]. The clean Cu(115) surface up to around 570 K is characterized by straight and equally spaced steps without reconstruction. Thermal roughening of Cu(115) takes place at temperatures lower than usually observed in the case of close-packed faces, *i.e.* just over 570 K (about $0.42T_{\mathrm{m}}$, where T_{m} is the melting point) [3, 4].

Structural aspects of alkali metal adsorption on different metal surfaces have been reviewed by Diehl and McGrath [5]. Due to the physicochemical properties of potassium (*e.g.* melting point, $T_{\mathrm{m}} = 336.5$ K and a vapor pressure less than 1×10^{-10} Torr below 530 K) its condensation on metal substrates is restricted to low temperature below *c.a.* 200 K. At a temperature of 200 K, greater than half of the melting point, a rapid approach to thermodynamic equilibrium on the surface is expected. On the Cu(011) substrate, the low temperature desorption peak observed at 330 K, is attributed to a potassium multilayer structure [6, 7]. Studies of potassium adsorption around room temperature (RT) are restricted to coverages up to around one atomic layer only. A deposited alkali metal can induce a substantial rearrangement of the topmost layer of the metal substrate. A well-known example is the alkali induced (1×2) or missing row reconstruction on fcc(011) surfaces (*e.g.* K/Cu(011) [8]). The mechanism of the transformation is ruled out by the local increase in adsorption energy and does not require a large mass transport in the surface. It was shown that adsorption of another alkali metal — cesium on Cu(115) at 300 K — induces double step reconstruction of the substrate for coverages close to a monolayer [9]. For the K/Cu(115) interface at 340 K, the double step reconstruction is parallel to the observed faceting, *i.e.* formation of large (114) facets at higher coverages [10].

* corresponding author; e-mail: pjg@ifd.uni.wroc.pl

In this paper, in the context of the adsorption properties, two basic interfaces, namely K/Cu(115) and CO/Cu(115) were re-examined carefully. Recognition of their geometric and electronic properties is important for further investigations of coadsorption systems. The influence of crystallographic steps and alkali modification on coadsorption phenomena will be found in a coming study based on detailed knowledge of simple, elemental systems.

2. Experimental

Synchrotron radiation photoelectron spectroscopy (SR-PS) was performed at the SuperESCA beamline at ELETTRA (Trieste, Italy) using the ultrahigh-vacuum (UHV) chamber described elsewhere [11, 12]. Complimentary measurements using low energy electron diffraction (LEED) and X-ray photoelectron spectroscopy (XPS) were carried out at an auxiliary UHV system. During experiments the working pressure in both apparatus was below 1.00×10^{-10} Tr.

The Cu(115) crystal, mounted on the manipulator, could be cooled down to *c.a.* 120 K and heated to 900 K. The heating procedure was accomplished by passing a DC current through the sample holder. The temperature of the sample was measured by a chromel–alumel (type K; nickel–chromium and nickel–aluminium alloys of nominal composition of $Ni_{90}Cr_{10}$ and $Ni_{94}Mn_4Al_2Si_1$, respectively) thermocouple fixed to the top of the specimen. The UHV cleaning included cycles of Ne^+ ion bombardment (1200 eV, 1 μA, 5 min.) and annealing at 900 K (1–2 min.) in order to remove implanted neon ions and reduce damages introduced by gas bombardment. The procedure (several cycles) was prolonged until no contamination of the surface could be observed by photoemission.

Potassium was dosed to the front of the sample surface from a degassed chromate dispenser (SAES Getters) similarly as described previously [13]. Preliminary evaluation of the source showed that one adsorbate monolayer (AML) could be obtained after 40–50 s of deposition, *i.e.* the flux was approximately of 4/3 AMLs/min. The growth rate is considered here as a quite big flux of impinging potassium atoms but the condensation process seems to be performed at near stable (equilibrium) conditions at the applied temperatures. High purity CO gas was introduced through an inlet system and exposures were calculated by taking into account the indication of the ion gauge and expressed in langmuirs (1 L corresponds to the admission of 1.00×10^{-6} Tr by one second).

Work function changes, $\Delta\Phi$, were determined by measuring photoelectrons in an energy interval around the low energy cut-off (see the left part of Fig. 1). For a well-defined determination of the cut-off energy, the sample was biased at -9.0 V using an external battery.

Experimental photoelectron spectra were carefully analyzed taking into account procedures for elimination of

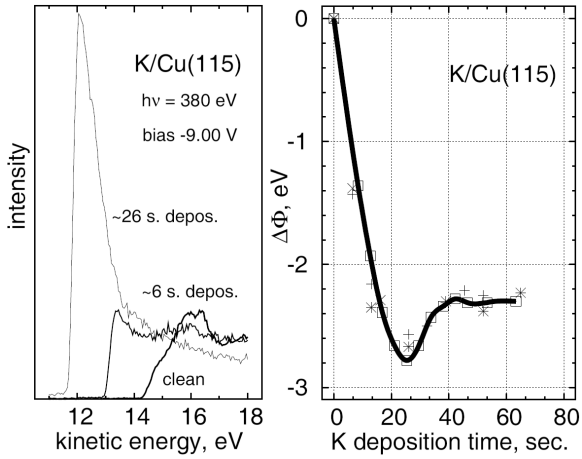

Fig. 1. Left side: Typical examples of photoelectron energy distributions ($h\nu = 380$ eV) used for determination of work function changes obtained from clean and potassium covered Cu(115). Right side: Work function changes, $\Delta\Phi$, of selected experiments showing the influence of the quality of the investigated interface on the minimum and saturation levels derived using the energy cut-off method.

uncertainties [14]. The secondary continuous spectrum and the peaks were fitted with the help of a Shirley-type background line and the asymmetric Gaussian–Lorenzian sum function. The K $2p$ spectrum ($2p_{3/2}$ and $2p_{1/2}$) obtained with the X-ray of Mg K_α ($h\nu = 1253.6$ eV) showed a binding energy position of around 296.5 eV with the spin orbit splitting value equal 2.76 eV and the Gaussian to Lorenzian ratio about 50:50. It is assumed that the area under the total feature corresponds to the intensity of the photoelectron transition.

3. Results

3.1. K/Cu

The change in the work function of potassium adsorbed at low temperature, $T = 130$ K, on Cu(115) is shown in Fig. 1. To illustrate the measurement method, the initial part of selected electron energy distribution curves (for $h\nu = 380$ eV) are drawn on the left side of the figure. The points showed on the right side of the graph, coming from several experiments and performed in different vacuum systems, are plotted as a function of deposition time. In different series of measurements (with reduced flux value) the time of deposition was normalized according to the work function minimum and the time used in the LEED and the K $2p$ intensity measurements. The thick line represents the $\Delta\Phi$ trend. The results show the typical behavior of alkali metal growth on a metal substrate, *i.e.* at first $\Delta\Phi$ decreases, goes through a minimum and then increases to a saturation level. For the interface under investigation, the maximum work function shift is equal to $-2.78(7)$ eV and the saturation level to $-2.31(7)$ eV. Uncertainty was determined taking into

account the results obtained in several different measuring systems. The point in which the $\Delta\Phi$ curve reaches a saturation level could be assigned to the coverage corresponding to a first complete potassium layer on Cu(115). According to the data, the minimum of the work function appears at the potassium coverage equal to 0.60(1) monolayer.

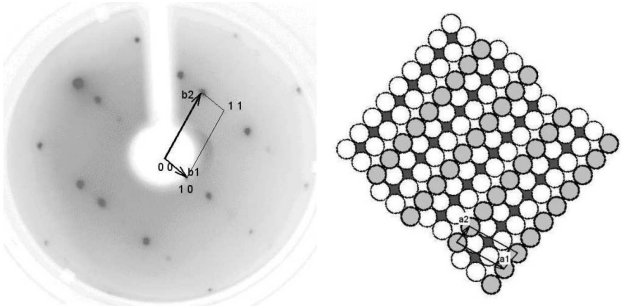

Fig. 2. Left side: LEED pattern (negative) recorded at a primary beam energy of 183 eV from the clean Cu(115) substrate at 425 K. Right side: hard-sphere model of the unreconstructed Cu(115) surface.

The clean Cu(115) stepped surface shows the LEED pattern, Fig. 2, with the paralleogram-shaped reciprocal unit cell corresponding to an unreconstructed substrate. The geometric spot positions reflect the arrangement of the atomic cores of the top layer. The stepped Cu(115) surface consists of (001) terraces, three atoms rows wide (Table I) [2, 9, 18], and has a density of surface atoms greater than the one of the Cu(001) surface.

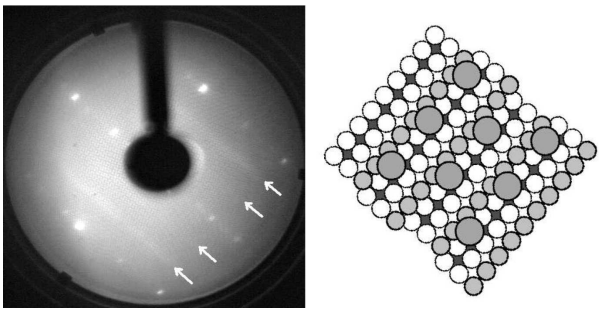

Fig. 3. Left side: LEED pattern obtained after 40 s of potassium adsorption on the Cu(115) substrate at 125 K; the primary beam energy is 178 eV. The arrows indicate the directions on which the adsorbate-induced extra spots are present. Right side: hard-sphere model of the K/Cu(115) interface, the quasihexagonal structure on an unreconstructed substrate (QHU).

LEED patterns of low temperature (125 K) potassium adsorption shows appearance of the diffused streaks appearing at approximately 1/3 position with respect to perpendicular direction to the [010], increase of the background level (Fig. 3, left side) and finally the mixed structure with the high background. The streaks are characteristic of a poor ordering of the chains and the

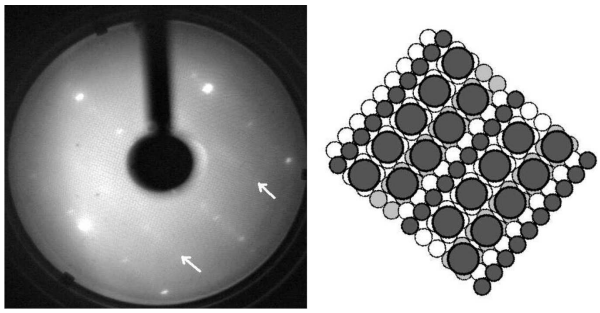

Fig. 4. Left side: LEED pattern obtained after 32 s of potassium adsorption on the Cu(115) substrate at 425 K. The primary beam energy is 105 eV. The (2×2) superstructure could be clearly identified. The arrows indicate the directions on which the adsorbate-induced extra spots are present. Right side: the suggested model for the first potassium monolayer on Cu(115) at 425 K, named missing double rows reconstruction (MDR), corresponding to the (2×2) pattern.

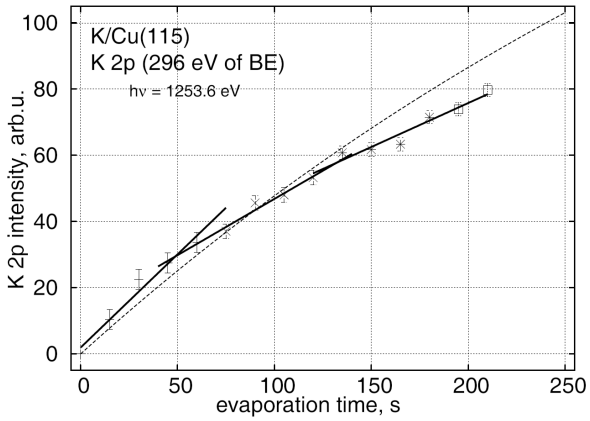

Fig. 5. Intensity of the K $2p$ photoelectron (XPS) as a function of potassium deposition time on the Cu(115) surface at 125 K. The broken line is constructed on the base of regression analysis of the successive parts of the data. The dashed line corresponds to the evaluated dependence of the layer-by-layer growth mode.

pattern can be explained in terms of K atom rows positioned along step edges. No evidence of reconstruction was found at that temperature of adsortpion for all coverages. The background level of the diffraction image reflects a poor ordering of the potassium layer which is a consequence of reduced adatom mobility at low temperature. The regions where the K atoms are not ordered coexists with ordered domains. A model of the interface includes chains of K adatoms which could be slightly compressed along the step edge direction (LCU) or eventually create zig-zag chains (ZCU) of higher density. It is worth to mention that a quasihexagonal arrangement of the K atoms within the troughs provided by the Cu substrate (QHU) of a density of 2.0×10^{18} at/m^2 could not be excluded at the beginning of adsorption (Fig. 3, right side). A *bcc* structure of bulk potassium has a unit

cell with $a = 532.8$ pm and the closest K–K separation as $a(3/2)^{1/2} = 461.4$ pm [15]. Accordingly, a density of the most dense K(011) plane is equal to 4.98×10^{18} at/m^2. The density of the linear (LCU) and zig-zag (ZCU) arrangements on an unreconstructed substrate could be calculated as $(664.1 \times 461.4)^{-1} = 3.26 \times 10^{18}$ at/m^2 and $(664.1 \times 414.5)^{-1} = 3.63 \times 10^{18}$ at/m^2, respectively, *i.e.* 66% and 73% of the the K(011) plane density. After 24 s of adsorption of potassium at 425 K the background increases and streaks mainly at the position between direction of $\boldsymbol{b_1}$ are clearly observed. The streaks in halfway between the integer beams develop into (2×2) structure after 32–40 s of deposition (Fig. 4, left side). Then, the background intensity increases continuously with the time of adsorption. The (2×2) structure is identified as the missing double rows (MDR) reconstruction, namely every other Cu atom double row is missing. K adatoms form double chains located between the remaining rows on the substrate. A structural model of the interface is presented in Fig. 4 (right side) for which the full interface layer density is calculated as $(2.9\text{–}3.3) \times 10^{18}$ at/m^2. The presence of a high background indicates that the reconstruction is a local process which starts by the formation of small reconstructed nuclei. It should be mentioned that the exact position of the atoms within the unit cell could be not determined by the present LEED investigations.

TABLE I

Crystallography data of selected ideal copper surfaces: fcc lattice constant of 361.49 pm ($p = 1 \times 10^{-12}$); Cu–Cu bond length of 255.6 pm [15]. N/UC is the number of atoms per unit cell and TW is the terrace width. The surface density of atoms was calculated taking into account indicated N/UC despite of the "corner" atoms (below the step) are not wholly accessible. 1×10^{18} at/m^2 $= 1 \times 10^{14}$ at/cm^2.

copper surface	basic vectors			N/UC	TW [pm]	surface density [at/m^2]
	angle	a_1 [pm]	a_2 [pm]			
(001)	90°	255.6	255.6	1	∞	15.31×10^{18}
(115) or 3(001) × (111)*	79.11°	255.6	676.3	3	664.1	17.67×10^{18}
(119) or 5(001) × (111)*	83.70°	255.6	1171	5	1164	16.81×10^{18}

*compact step notation [16, 17].

Due to intrinsically smaller signals, the conversion of photoelectron intensities to atomic concentrations involves greater uncertainty than in the case of electron-excited Auger electron spectroscopy. Despite of that, plot of the intensities (as measured peak areas) with deposition time could be used as the method for determination of the condensate growth mode (*e.g.* [19]). The condensate photoelectron intensity I as a function of the film thickness, expressed in (adsorbate) monolayers, n, follows according to the formula: $I(n) = I(\infty)[1 - \exp(-n/\lambda_{\mathrm{ED}})]$, where $I(\infty)$ denotes the intensity of the bulk condensate and λ_{ED} is the electron escape depth. Rearranging the relation to the values for $n = 1$ and 2, it can be obtained: $I(\infty) = [I(1)I(1)]/[2I(1) - I(2)]$; and $\lambda_{\mathrm{ED}} = (\ln(I(1)/[I(2) - I(1)]))^{-1}$. Plot of the K $2p$ intensity I (expressed in arbitrary units (arb.u.)), as a function of heating time of the potassium source (s) obtained during adsorption at 125 K is presented in Fig. 5. The data are scattered and to establish a reliable evaluation the self-consistent method was adopted. Using a linear regression procedure to the successive parts of points, the plot is approximated by a broken line. First break is found after 50 s of deposition and corresponds to a K $2p$ intensity of 29.8 arb.u. The values of the second break are: 130 s and 56.10 arb.u., respectively. Introducing the values into the above mentioned equations, under the assumption that the breaking points correspond to complete layers, the bulk potassium intensity, $I(\infty)$, is calculated as 254 arb.u. and the electron escape depth of electrons of 957 eV kinetic energy is 8.00 adsorbate monolayers, AML. The calculated value of the $\lambda_{\mathrm{ED}}(957)$ through potassium layers using the Seah–Dench formula with an average potassium layer thickness of 422.7 pm is equal to 8.25 AML [20] and according to the Cumpson–Seah equation (without approximation concerning the layer thickness) is 6.84 AML [21].

The time of the second break 130 s is greater than the time of the first break 50 s. It could be a consequence of decreasing sticking coefficient of potassium to the changed interface and/or greater atomic density of the second layer. Potassium adatoms in the first adlayer are most probable arranged in the simple (linear) or zig-zag chains of atoms along the steps. The above found densities represent 65% and 73% of the density of the

K(011) plane and could be compared with the first to second break time ratio of 0.63. It is concluded that the density effect during potassium adsorption is dominating. The positions of the remaining points of the K $2p$ intensity under the theoretical curve are characteristic for the $3D$ islands growth over the completed two monolayers. Adsorption proceeds through filling of the substrate surface rows (first layer, less dense), then build up of second layer (more dense), and finally the spread of the points reflects $3D$ islands growth.

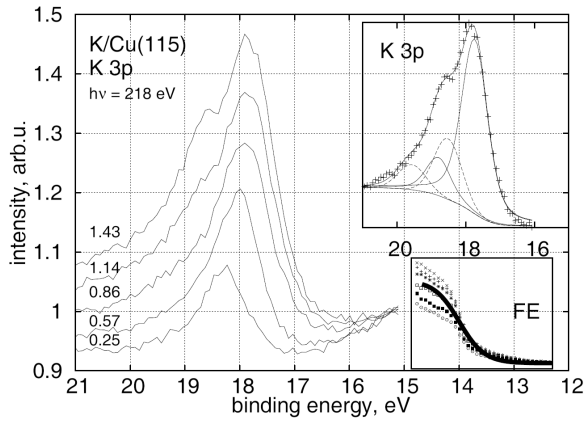

Fig. 6. Typical examples of the K $3p$ photoelectron spectrum (SR-PS). The potassium coverage (adsorbate monoalyers) is the parameter of the curve. Right side: details of the peak analysis (top inset) and (bottom inset) the Fermi edge determination for the whole set of data.

The K $3p$ peak is positioned in the valence band spectra at around 18 eV below the Fermi level. Several chosen spectra of the K $3p$ for different coverages are shown in Fig. 6. The top inset shows the example of a synthesis of the peak for a coverage greater than one complete potassium layer. In the bottom inset, the procedure of the Fermi edge determination is illustrated as the average of all involved spectra. The K $3p$ feature is relative broad and the maximum shifts towards smaller binding energy with increasing coverage in correlation with the work function changes. This large linewidth is due to vibrational broadening and probably to an interatomic processes connected with its huge increase of intensity following gas adsorption. Those effects suppress the sharpness of the peak and the $p_{3/2}$-$p_{1/2}$ spin-orbit splitting, usually accepted as 0.24 eV [22, 23] cannot be resolved. The K $3p$ peak shows two satellites which are drawn in the inset of Fig. 6 as the dashed lines. At low K coverage a satellite is positioned at 0.85 eV and with the coverage its intensity slightly increases up to around 30% of the main line. The second satellite, appearing at higher coverages, is shifted 1.77 eV below the main line. For the noticed shoulder in the rough spectrum, the second feature is responsible and it originates from the surface contribution. The surface peak, more sharp than the interface peak, appears after completion of the first potassium layer on the substrate. The satellites correspond to a single ion $4s$ shakeup process and interband transitions involving the $4s$ band of the dense potassium layer. The K $3p$ core level is indicative for determination of the potassium coverage on the copper surface.

3.2. CO/Cu

It is worth to point out that usually CO adsorption on metals induces an increase of the work function except for platinum and group Ib metals. It was found that during CO adsorption at low temperature ($\approx$ 80 K) on the three basic copper surfaces, the work function decreases through a minimum, approximately of $-$(0.30–0.50) eV and saturates below the starting value by $-$(0.10–0.20) eV [24]. Concerning the investigated Cu(115) surface, the $\Delta\Phi$ with CO exposure at $T = 130$ K shows a similar shape as is published for Cu(001), with a minimum around -0.30 eV. The final (unchanging) value of $\Delta\Phi$ of around -0.20 eV is detected after 1.50 L dose of carbon monoxide and this dose is taken as the saturation of CO adsorption. The reduction of $\Delta\Phi$ is explained on the basis of the charge transfer from the CO 5σ orbital to the copper $3d$ band.

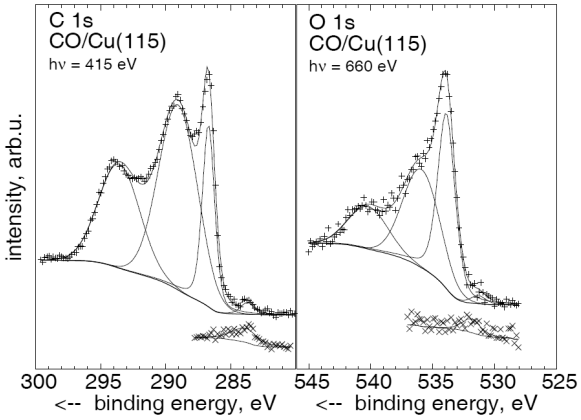

Fig. 7. Synthesis of the C $1s$ and O $1s$ photoelectron spectra (SR-PS) obtained after saturation of the Cu(115) surface with CO at $T = 130$ K. Bottom spectra corresponds to the interface after annealing to 223 K.

Continuous registration of the C $1s$ and O $1s$ regions during CO adsorption shows uniform increase of the core level spectra which contain the triplet structures (Fig. 7). From whole measurements it is seen that the features in both regions correspond to the one adsorption state of carbon monoxide on Cu(115). Corresponding to the saturated CO layer, the spectra consist of the main $1s$ peak and two satellites separated by +(2.0–2.3) eV and +(6.3–6.9) eV for carbon and oxygen peak, see Tables II and III, respectively. The satellites, assigned to many-electron processes, are characteristic for chemisorbed carbon monoxide [26, 28]. Relative intensities of the main peaks are estimated as *c.a.* 18% and 40% of the total areas under the features for C $1s$ and O $1s$, respectively.

TABLE II

Experimental data of the C 1*s* peak position of indicated species. BE — binding energy relative to the Fermi level (to the vacuum level, where indicated by VL) in eV; fwhm — full width at half maximum in eV; I(rel) — relative intensity (area), %; g — gas phase.

Interface	residual	main		1st satell.		2nd satell.	
	BE/fwhm	BE/fwhm	I(rel)	BE/fwhm	I(rel)	BE/fwhm	I(rel)
CO (g) [25]		295.9_{VL}/0.71					
CO_2(g) [25]		297.5_{VL}					
CO/Cu poly				M + 2.8		M + 7.4	
77 K [26]		286.6	29	289.4	51	294.0	21
CO/Cu(001)							
80 K [27]		286.3					
CO/Cu(115)				M + 2.31		M + 6.91	
130 K	283.71/1.22	286.70/1.12	18.4	289.03/3.54	50.5	293.56/3.71	29.8
CO/Cu(115)							
220 K	283.87/2.36						
diamond [25]		283.5					
graphite [25]		284.3–284.7					

TABLE III

Experimental data of the O 1*s* peak position of indicated species. BE — binding energy relative to the Fermi level (to the vacuum level, where indicated by VL) in eV; fwhm — full width at half maximum in eV; I(rel) — relative intensity (area), %; g — gas phase.

Interface	residual	main		1st satell.		2nd satell.	
	BE/fwhm	BE/fwhm	I(rel)	BE/fwhm	I(rel)	BE/fwhm	I(rel)
O_2(g) [25]		543.1_{VL}					
CO(g) [25]		542.1_{VL}/0.56					
CO_2(g) [25]		540.8_{VL}					
CO/Cu poly				M + 2.9		M + 7.3	
77 K [26]		533.7	30	536.0	46	541.0	24
CO/Cu(001)							
80 K [27]		533.0					
CO/Cu(115)				M + 2.01		M + 6.32	
130 K	531.31/1.45	533.89/1.66	39.7	535.90/3.50	40.2	540.21/3.74	18.5
CO/Cu(115)							
220 K	531.90/2.29						
Cu_2O [25]		530.4					

The satellites are more pronounced for carbon than oxygen and the width of the C 1*s* peak is smaller than the one of the O 1*s*. The binding energy of the main peak (lowest BE) can be used as a fingerprint for the adsorbed state of CO. In Table II and Table III, the binding energies of the 1*s* peak corresponding to different substances are collected as well. It is calculated that the binding energy of the C 1*s* peak shifts approximately by −6 eV relative to CO gas phase (after subtraction of the typical work function from the VL value) upon CO chemisorption on Cu(115). Similar considerations of the binding energy of the O 1*s*, shows the shift of the main peak to be −4 eV relative to the gas phase. After heating the CO/Cu(115) interface to 220 K, small broad features at 283.87 and 531.31 eV are noticed in the spectra which are attributed to residual carbon and oxygen of graphitic and oxide form, respectively. The binding energy positions indicate contaminating carbon on the metallic substrate and the oxide phase of copper. The C 1*s* and O 1*s* photoemission spectra obtained during the experiment are shown as the lowest part of the Fig. 7.

4. Discussion

The results concerning work function measurements are in good agreement with the reported values. The work function of potassium (bcc) polycrystalline, monocrystals with (001), (011) and (111) faces are published as corresponding to 2.22, 2.12, 2.54 and 2.35 eV, respectively [29]. Assuming the work function of the Cu(115) surface as 4.75 eV (close to the Cu(001) surface) or slightly higher, the saturation value is obtained as 2.44 eV, which is very close to the value of the most dense potassium surface. From the slope of the $\Delta\Phi$ curve it could be concluded that potassium shows ionic behavior in the region up to 2 doses (30% of the first layer). The adsorbate becomes more metallic and could be interpreted as pure metallic after 4 doses (60% of first layer). Concerning the quality of the investigated surface, a valuable information is provided by the work function measurements. The interface cleanliness before and after alkali deposition could be very well checked using the minimum and the saturation values. Unwanted adsorption of residual gases and contaminations increases the value of the work function and consequently reduces the depth in the $\Delta\Phi$ relation. The values obtained in the present experiment are representative of very clean adsorption processes. Secondly, it is worth to note that the $\Delta\Phi$ value could be used for a precise determination of the potassium coverage.

Initial adsorption of potassium represents ionic adsorption with the negative charge shift towards the substrate. Despite of the smaller adsorbate feature (ionic radius of K is smaller than atomic one), which could lead to the building of a very dense overlayer, the adatomic distances at the real adlayer are still large due to the repulsive interaction. That is why the identification of the QHU structure at low coverages is not surprising. The more packed layer is formed when the repulsive interaction becomes smaller, *i.e.* when the adsorbate will change its character towards a more atomic one (less ionic). Simply, due to definitely greater size of the adsorbate over substrate, lateral interaction (in-the-layer) is substantiated over the steps at the interface. It is clear, that influence of the substrate geometry still exists and it is directed to creation of the dense zig-zag channels. Under assumption of metallic radius of potassium, the coverage corresponding to the zig-zag channels are calculated as being in the interval of 65–73% relative to the K(011) surface layer. The low temperature adsorbate monolayer was a compressed chain of potassium atoms on the unreconstructed substrate (CCU) and assuming the nearest K–K distance to be 0.43 nm (which is characteristic for the K/Cu system), the corresponding density is equal to 3.51×10^{18} at/m^2.

A simple criterion, taking into account the surface free energies γ_{K} and γ_{Cu} and the interface energy γ_i at the boundary of the two metals, allows a rough indication of the growth mode. The interfacial energy, γ_i, could be estimated from the relevant Miedema's formula, $\gamma_i = (\sqrt{\gamma_{\mathrm{K}}} - \sqrt{\gamma_{\mathrm{Cu}}})^2$ with $\gamma_{\mathrm{K}} = 0.15$ J/m^2 and $\gamma_{\mathrm{Cu}} = 1.85$ J/m^2 [30]. Comparison of the sum of the $\gamma_i + \gamma_{\mathrm{K}}$ with the γ_{Cu} shows that $\gamma_i + \gamma_{\mathrm{K}} < \gamma_{\mathrm{Cu}}$, which in turn predicts a wetting of the substrate by potassium leading to Stranski–Krastanov (three-dimensional islands over complete layer) growth mode [31].

Analysis of the low temperature results of the used methods show that potassium in the first layer at low coverages occupies the edges of the terrace copper sample. Due to some degree of charge transfer to the substrate, before the minimum at $\Delta\Phi$, creation of the quasi-hexagonal adsorbate structure is induced by lateral interaction of long-range. It is worth to point out that the distances between the adsorbate units having partly ionic character are not influenced by the substrate periodicity. Compression of the linear chains towards zig-zag chains at the interface accompanies an increase in work function from the minimum to the saturation level. As a consequence, the first created layer has a coverage not exceeding *c.a.* 70% of the K(011) density. On the other hand, the adatom density in the second layer is very close to the density of bulk potassium.

Potassium adsorbed at higher temperatures is restricted to one complete layer which is formed during reconstruction of the substrate. The heat of sublimation of alkali metal is too small to allow an easier growth of multilayers a RT.

Work function changes of CO adsorption are not so pronounced as in the case of an alkali metal, however the shape of the $\Delta\Phi$ curve is similar. The decrease of the work function at the saturation coverage indicates charge transfer from the CO molecule to the substrate. Due to a similar value of $\Delta\Phi$ in the case of a Cu(001) substrate it is concluded that strictly "on top" surface states are occupied by CO molecules. CO molecules stick perpendicularly to the surface plane with the carbon atom placed down as usually takes place for most metal surfaces. Hence, the sites near the step edges are not occupied by molecules because of simple geometry size limitation.

The core level photoelectron spectroscopy is sensitive to the local geometry of adsorbed molecules. A good example is molecular adsorption of CO on Ni(001), where different adsorption sites were determined from measurements of the binding energy shifts. The following order of BE(ontop) > BE(bridge) > BE(hollow) was published with shifts of 0.8 and 0.3 eV for C 1*s* and 1.6 and 0.9 eV for O 1*s*, respectively [27]. It is explained on the basis of the statement: higher BE, weaker adsorbate–substrate interaction. This is not the case of CO adsorption on the Cu(115) surface where the adsorption behaviour is very similar to the CO/Cu(001) case. At the investigated adsorption temperature, the CO molecule is in a chemisorbed state. Conversion from physisorbed to chemisorbed state of CO was published as taking place at around 30 K for a copper substrate [26]. At small CO–CO distances, the interaction between the CO molecules is strongly repulsive which leads to creation of ordered layers on Cu(001). Then up to *c.a.* 150 K no change in

bonding mode occurs [26]. Concerning the interface under investigations, a multipeak structure of the core levels occur for one single adsorption state what was published in the past (*e.g.* [26, 27, 32]). Possible explanations of the structure include the shake-up transitions contributing to the two satellites observed at higher binding energy with respect to the main peak [32]. From a comparison of the main peak widths, the relation in the gas phase is opposite to the chemisorption on Cu(115). The larger broadening of the O 1*s* line, observed here, is caused by the C–O bond lenghtening in the adsorbed molecule.

In summary, the conclusions of the present study are:

1. K adatoms occupy the sites near the step edges of the substrate only. The work function minimum corresponds to occupation of all possible sites.

2. CO molecules adsorb with "on-top" position relative to the substrate atoms and interact with one copper atom only through carbon. Molecules keep off the places at the corner just below the next step of the substrate.

Acknowledgment

We appreciate support from The Danish Natural Science Research Council.

References

[1] G. Witte, J. Braun, A. Lock, J. Toennies, *Phys. Rev. B* **52**, 2165 (1995).

[2] F. Hofmann, U. Svenson, J. Toennies, *Surf. Sci.* **371**, 169 (1997).

[3] J. Lapujoulade, J. Perreau, A. Kara, *Surf. Sci.* **129**, 59 (1983).

[4] D. Gorse, J. Lapujoulade, V. Pontikis, *Surf. Sci.* **178**, 434 (1986).

[5] R. Diehl, R. McGrath, *Surf. Sci. Rep.* **23**, 43 (1996).

[6] M. Christiansen, E. Thomsen, J. Onsgaard, *Surf. Sci.* **261**, 179 (1992).

[7] L. Dubois, B. Zegarski, H. Luftman, *J. Chem. Phys.* **87**, 1367 (1987).

[8] R. Schuster, J. Barth, G. Ertl, R. Behm, *Surf. Sci.* **247**, L229 (1991).

[9] J. Braun, J. Toennies, G. White, *Surf. Sci.* **340**, 265 (1995).

[10] L. Schwenger, H.-J. Ernst, *Surf. Sci.* **347**, 25 (1996).

[11] J. Onsgaard, S. Hoffmann, P. Godowski, P. Moller, J. Wagner, A. Groso, A. Baraldi, G. Comelli, G. Paolucci, *Chem. Phys. Lett.* **322**, 247 (2000).

[12] J. Onsgaard, S. Hoffmann, P. Møller, P. Godowski, J. Wagner, G. Paolucci, A. Baraldi, G. Comelli, A. Groso, *Chem. Phys. Chem.* **4**, 466 (2003).

[13] P. Godowski, J. Onsgaard, S. Christensen, J. Nerlov, *Acta Phys. Pol. A* **89**, 657 (1996).

[14] S. Evans, *Surf. Interf. Anal.* **18**, 323 (1992).

[15] `http://www.webelements.com/` (2008).

[16] M.G. van Hove, G.A. Somorjai, *Surf. Sci.* **92**, 489 (1980).

[17] D. Eisner, T. Einstein, *Surf. Sci.* **286**, L559 (1993).

[18] H. le Rouzo, P. Parneix, G. Raseev, K. Smirnov, *Surf. Sci.* **415**, 131 (1998).

[19] M. Heuberger, G. Dietler, L. Schlapbach, *Surf. Sci.* **314**, 13 (1994).

[20] M. Seah, W. Dench, *Surf. Interf. Anal.* **1**, 1 (1981).

[21] P. Cumpson, M. Seah, *Surf. Interf. Anal.* **25**, 430 (1997).

[22] D. Riffe, G. Wertheim, P. Citrin, *Phys. Rev. Lett.* **64**, 571 (1990).

[23] G. Wertheim, D. Riffe, N. Smith, P. Citrin, *Phys. Rev. B* **46**, 1955 (1992).

[24] S. Ishi, Y. Ohno, B. Viswanathan, *Surf. Sci.* **161**, 349 (1985).

[25] T. Carlson, *Photoelectron and Auger Spectroscopy*, Plenum Press, New York 1975.

[26] P. Norton, R. Tapping, J. Goodale, *Surf. Sci.* **72**, 33 (1978).

[27] H. Antonsson, A. Nilsson, N. Mårtensson, I. Panas, P. Siegbahn, *J. Electr. Spectr. Rel. Phenom.* **54/55**, 601 (1990).

[28] O. Gunnarsson, K. Schönhammer, *Phys. Rev. Lett.* **41**, 1608 (1978).

[29] W. Fomienko, *Sprawocznik: Emissionnyje Swojstwa Matierialow*, Naukowa Dumka, Kijew 1981.

[30] A. Miedema, P. de Châtel, F. de Boer, *Physica B+C* **100**, 1 (1980).

[31] J. van der Merwe, *Prog. Surf. Sci.* **67**, 365 (2001).

[32] R. Messmer, S. Lamson, D. Salahub, *Solid State Commun.* **36**, 265 (1980).